PNAS RESEARCH ARTICLE | ECOLOGY OPEN ACCESS

Community assembly influences plant trait economic spectra and functional trade-offs at ecosystem scales

William R. L. Anderegg[a,b,1], Jordi Martinez-Vilalta[c,d], Maurizio Mencuccini[c,e], and Rafael Poyatos[c,d]

Edited by Susan Harrison, University of California Davis, Davis, CA; received February 28, 2024; accepted May 10, 2024

Plant functional traits hold the potential to greatly improve the understanding and prediction of climate impacts on ecosystems and carbon cycle feedback to climate change. Traits are commonly used to place species along a global conservative-acquisitive trade-off, yet how and if functional traits and conservative-acquisitive trade-offs scale up to mediate community and ecosystem fluxes is largely unknown. Here, we combine functional trait datasets and multibiome datasets of forest water and carbon fluxes at the species, community, and ecosystem-levels to quantify the scaling of the tradeoff between maximum flux and sensitivity to vapor pressure deficit. We find a strong conservative-acquisitive trade-off at the species scale, which weakens modestly at the community scale and largely disappears at the ecosystem scale. Functional traits, particularly plant water transport (hydraulic) traits, are strongly associated with the key dimensions of the conservative-acquisitive trade-off at community and ecosystem scales, highlighting that trait composition appears to influence community and ecosystem flux dynamics. Our findings provide a foundation for improving carbon cycle models by revealing i) that plant hydraulic traits are most strongly associated with community- and ecosystem scale flux dynamics and ii) community assembly dynamics likely need to be considered explicitly, as they give rise to ecosystem-level flux dynamics that differ substantially from trade-offs identified at the species-level.

Climate change | climate extremes | carbon cycle | functional traits

Plant trait economic spectra are widely used in ecology and often locate species on a "conservative-to-acquisitive" spectrum or trade-off of life history strategies whereby acquisitive species have high rates of resource acquisition, such as high maximum photosynthetic rates, but are less stress-tolerant in general, including during severe drought (1, 2). Plant traits are most commonly measured at a tissue or organism scale, but scaling up plant economic spectra traits and their inferences to species, community, and ecosystem scales is a fundamental goal of community and global ecology (3–5) and also thought to be key for understanding and projecting climate change impacts on terrestrial ecosystems (6–9). Yet, trait spectra and associated trade-offs have been shown to be scale-dependent when assessed within species (10), and scaling tissue/organism-level traits to capture trade-offs and dynamics at larger scales of organization is strikingly challenging, particularly in light of community assembly and species interactions (11, 12). Critical scaling questions include the following: i) How do traits mediate physiological and demographic outcomes, ii) what traits are most strongly associated with flux dynamics at community and ecosystem scales, and iii) how do species and trait diversity influence climate responses such as drought sensitivity at ecosystem scales? The plant economic spectra literature raises a major question: Does a conservative-acquisitive trade-off exist at ecosystem scales?

Recent work at the ecosystem scale using eddy covariance data has examined global variation in ecosystem flux dynamics (4, 13) but has generally not considered trait-mediated drought responses or trade-offs across multiple scales. We define ecosystem scales here as the measurement footprint of an eddy covariance tower (typically ~10^5 to 10^7 m^2 in forests, depending on tower height, wind, and other conditions), which estimates carbon and water fluxes in that footprint using concurrent water and carbon concentrations and wind speed and direction measurements. Notably, the central axes identified at ecosystem scales actually indicate that conservative water strategies are largely decoupled from (e.g., orthogonal to) acquisitive carbon strategies (4), which is at odds with plant economic spectra literature that finds strong trade-offs among these traits at tissue or individual scales (1, 2, 14). Understanding how traits mediate the scaling of life history strategies and trade-offs is critically important for ecosystem and carbon cycle models, including their ability to project the impacts of climate change and the potential for carbon cycle feedbacks to accelerate climate change.

Significance

The responses of forests across the globe to climate change remain uncertain. Plant functional traits may help improve ecosystem model projections of climate impacts, but which traits mediate climate responses from species to ecosystems remains poorly understood. We quantify whether the fundamental trade-off between fast resource acquisition and stress tolerance occurs at species, community, and ecosystem scales. We find that the trade-off weakens at ecosystem scales and this weakening appears to be due to the combinations of traits of species found in these communities and ecosystems. These findings indicate that ecosystem models may need to include more realistic combinations of species and their water transport traits to better simulate the future of forests in a changing climate.

Author affiliations: [a]Wilkes Center for Climate Science and Policy, University of Utah, Salt Lake City, UT 84103; [b]School of Biological Sciences, University of Utah, Salt Lake City, UT 84103; [c]Ecological and Forestry Applications Research Centre (CREAF), Bellaterra (Cerdanyola del Vallès), Catalonia E08193, Spain; [d]Department of Animal Biology, Plant Biology and Ecology, Universitat Autònoma de Barcelona, Bellaterra (Cerdanyola del Vallès), Catalonia E08193, Spain; and [e]Institució Catalana de Recerca i Estudis Avançats, Barcelona, Catalonia E08010, Spain

---

Author contributions: W.R.L.A., J.M.-V., M.M., and R.P. designed research; W.R.L.A. and R.P. performed research; J.M.-V., M.M., and R.P. contributed new reagents/analytic tools; W.R.L.A. analyzed data; and W.R.L.A., J.M.-V., M.M., and R.P. wrote the paper.

The authors declare no competing interest.

This article is a PNAS Direct Submission.

[1] To whom correspondence may be addressed. Email: anderegg@utah.edu.

This article contains supporting information online at https://www.pnas.org/lookup/suppl/doi:10.1073/pnas.2404034121/-/DCSupplemental.

Published June 21, 2024.

The disconnect between ecosystem-level responses and trade-offs identified at the species-level may be mediated by how community assembly processes affect the scaling of plant economic trade-offs from species to ecosystems. Community trait composition, including trait means and SD or dispersion of traits, have been widely used to test the role of niche processes (e.g., environmental filtering, niche partitioning) and neutral dynamics (e.g., dispersal limitations) within and across communities (15–17). However, a widely recognized challenge is that community assembly processes are inherently scale-dependent (15–21). This scale-dependence makes it challenging to theorize and directly test the relative importance of key community assembly processes across different scales from a species to a community (e.g., forest plot) to an ecosystem scale (e.g., flux tower footprint). Kraft and Ackerly (22) hypothesize that as scale expands to include more environmental heterogeneity, such as habitat type, soil patches, and microsites, environmental filtering is likely to drive increased trait diversity, which would likely lead to a buffering effect in a conservative-acquisitive trade-off because different species exhibit differential slopes on a trade-off between resource acquisition and stress response (Fig. 1) (9). Finally, the community assembly literature exploring the trait composition of the community must be integrated with the broad biodiversity–ecosystem stability and synchronicity literature to derive hypotheses for how traits influence carbon and water flux dynamics at community and ecosystem scales (e.g., refs. 9, and 23–27). In particular, we hypothesize that one of the major potential drivers of stability—asynchrony of species' responses due to differences in their intrinsic sensitivities to environmental fluctuations (27)—could combine with the environmental filtering across increasing environmental heterogeneity (22) and niche partitioning between canopy and understory to weaken the conservative-acquisitive trade-off in moving from community to ecosystem scales (Fig. 1).

While ecosystem models are crucial tools for scaling up tissue-level physiology to larger organizational scales and play a central role in future projections of terrestrial ecosystems and carbon cycle feedback (8), current global models generally do not include most community assembly processes such as environmental filtering or dispersal limitations that mediate ecosystem functional diversity (28). The future of the terrestrial carbon sink in a rapidly changing climate is highly uncertain (29, 30) and leveraging functional traits to better represent plant physiology, such as the physiology of plant water (hydraulic) transport, has been proposed as a major avenue for improving ecosystem models (9, 31, 32). While a broad body of literature has worked to improve physiological realism in these models, community assembly processes have received less focus (but see ref. 33) and are increasingly feasible to tackle with recent demographic ecosystem models (8). A foundation to these efforts to improve ecosystem models is a data-driven understanding of when and where species traits are useful for scaling to ecosystem responses and the degree to which community assembly processes mediate that scaling.

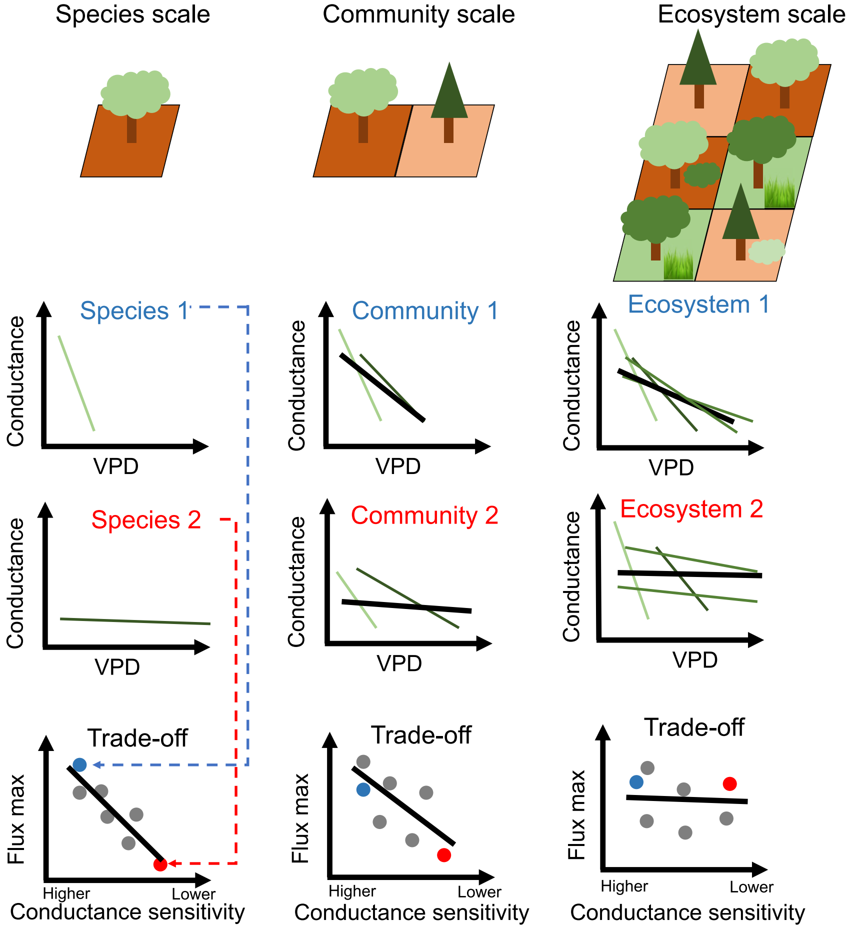

Fig. 1. Environmental filtering across a gradient of increasing environmental heterogeneity (per ref. 22) moving from species to community (i.e., dominant tree species within a forest stand) to ecosystem (i.e., flux tower footprint). Ground colors indicate environmentally differing patches; tree colors indicate different species or traits; and grass and shrubs show the inclusion of understory fluxes at ecosystem scales, which could further buffer fluxes through niche partitioning. Graphs show a hypothesized weakening in the trade-off between maximum fluxes (resource acquisition) and conductance sensitivity (stress tolerance) at different scales (green colors are individual species; the black line is overall average response in a community or ecosystem).

Here, we combined multibiome datasets of functional traits and water and carbon fluxes from sap flux and eddy covariance data [SAPFLUXNET (34) and FLUXNET2015 (35)] that covers scales of individual trees to forest ecosystems to ask: 1) How do conservative-vs-acquisitive trade-offs (plant economic spectra) scale from individual species to communities to ecosystems? 2) Which plant functional traits matter at ecosystem scales for predicting flux maximums and responses to atmospheric drought stress [vapor pressure deficit, VPD, a key stressor for forests that is increasing globally (36)]? 3) Does species diversity or trait diversity (e.g., resulting from community assembly) weaken/decouple these trade-offs at large scales and by what mechanism?

Results and Discussion

We quantified at each scale (species, community, or ecosystem) the level of "acquisitiveness" using the 90th percentile water flux rate during active seasons (see *Methods* for full details), akin to the maximum photosynthetic flux rate frequently used at leaf scale in plant economic spectra (2, 6, 14), and that scale's level of "stress tolerance" using the coefficient of response between canopy conductance and VPD following common practice at the species-level in the literature, where higher sensitivity is interpreted as lower drought tolerance (24, 25).

We found a strong conservative-acquisitive trade-off at the scale of individual species ($R^2 = 0.58$, $P \ll 0.0001$) but this trade-off weakened when scaling up to community ($R^2 = 0.48$, $P < 0.0001$) and almost disappeared at ecosystem scales ($R^2 = 0.09$, $P = 0.053$) (Fig. 2). Angiosperm and gymnosperm species or communities exhibited similar patterns in a conservative-acquisitive trade-off, but at the ecosystem scale, only gymnosperm-dominated eddy covariance sites showed a significant trade-off ($R^2 = 0.26$, $P = 0.01$; Fig. 2*C*). We compared a broad number of other metrics to capture this conservative-acquisitive trade-off, including carbon fluxes and coefficients that accounted for soil moisture and found broadly similar patterns (*SI Appendix*, Figs. S1 and S2). Our results revealed that a strong trade-off at the species-level, consistent with the plant economic spectra literature (1, 2, 6), largely disappears by the ecosystem-level, consistent with recent ecosystem analyses (4).

We then used univariate regressions between community-weighted mean and SD of functional traits and the above metrics of the conservative-acquisitive trade-off to illuminate which traits matter at community and ecosystem scales for explaining maximum flux rates and flux sensitivity to VPD. We found that different sets of functional traits underpin max fluxes versus sensitivities at community and ecosystem scales (Fig. 3). Broadly, plant hydraulic traits—including the water potential at 50% loss of stem conductivity (P50) and the hydraulic safety margin (HSM)—were more important than more traditional leaf or wood economic spectra traits, such as specific leaf area (SLA) or wood density (WD) (Fig. 3), consistent with recent studies (9). More negative community-weighted mean P50 was significantly associated with lower max flux rates at both scales (Community $P_{\mathrm{adj}} \ll 0.0001$, Ecosystem $P_{\mathrm{adj}} = 0.004$) and lower sensitivity to VPD at the community scale ($P_{\mathrm{adj}} \ll 0.0001$, Fig. 4), which is broadly consistent with the key role of plant hydraulics in mediating a trade-off between transport safety and efficiency. The community-weighted mean SLA was significantly correlated with maximum water fluxes at community ($P_{\mathrm{adj}} < 0.0001$) and ecosystem ($P_{\mathrm{adj}} = 0.027$) scales with higher SLA associated with higher water flux rates (Fig. 4), consistent with theory. We posit that the relationships between community-weighted traits and ecosystem flux responses documented here provide useful diagnostics or relationships for mechanistic models to capture.

Crucially, these univariate trait-flux relationships confirm that functional traits can "scale up" to explain and mediate community and ecosystem flux responses and reveal which traits are most relevant to which response processes. Community-weighted mean P50 was the trait most strongly associated with maximum fluxes at community and ecosystem scale, with community-weighted SLA emerging as the second-most important trait (Fig. 3). Both community-weighted mean and SD traits, particularly P50 and HSM, were associated with community flux variation, highlighting that both the species pool (trait mean) and trait diversity (trait SD) are likely important at these larger scales. Furthermore, the variance explained by important traits was generally substantially larger than species richness or clade (Fig. 3), further underscoring the utility of functional traits at large scales. At both scales, the variance explained by traits was generally substantially larger for

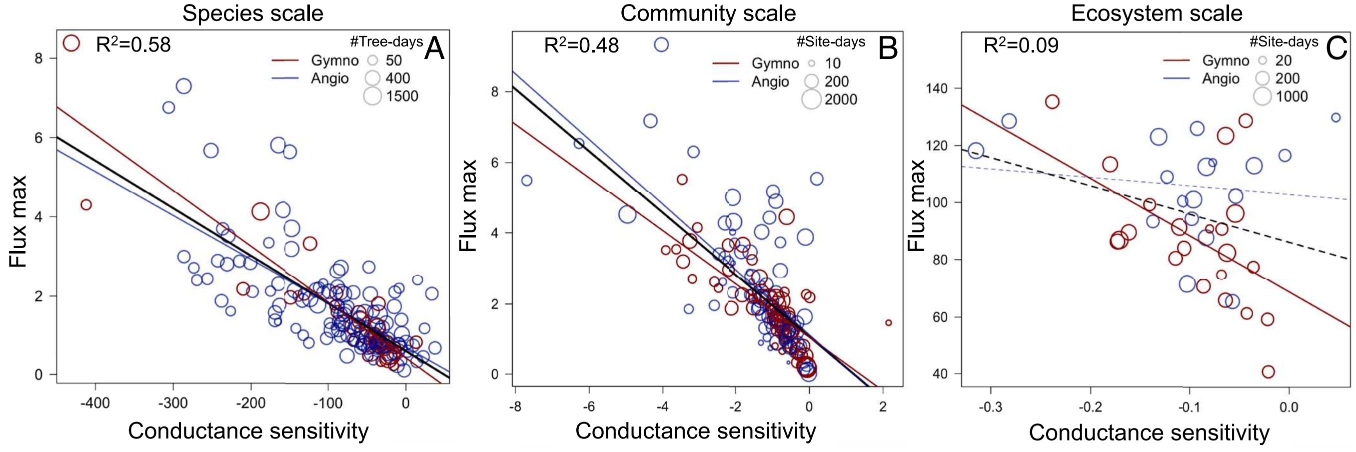

Fig. 2. Conservative-acquisitive trade-offs weaken from species to ecosystem scales. Relationships between the sensitivity of canopy or ecosystem conductance to VPD vs. the maximum water fluxes for species (*A*), community (*B*), and ecosystem (*C*) scales. Species and community scale fluxes and conductances are derived from SAPFLUXNET data and ecosystem fluxes and conductances from FLUXNET2015 data. Maximum water flux units are average daily cm^3 water/cm^2 sapwood area (*A*), mm/d (*B*), and average daily W/m^2 ground area latent heat fluxes (*C*), and conductance sensitivity units are mol water/(m^2 s log(kPa)) (*A*), mm/(day log(kPa)) (*B*), and mol water/(m^2 s kPa) (*C*). Blue circles indicate angiosperm species or angiosperm-dominated sites and the blue line is the ordinary least squares regression for those species/sites. Red circles indicate gymnosperm species or gymnosperm-dominated sites and the red line is the ordinary least squares regression for those species/sites. The black line is all species/sites. Solid lines indicate statistically significant and dashed lines nonsignificant relationships. Circle size is proportionate to the number of tree-days or site-days for each species/site.

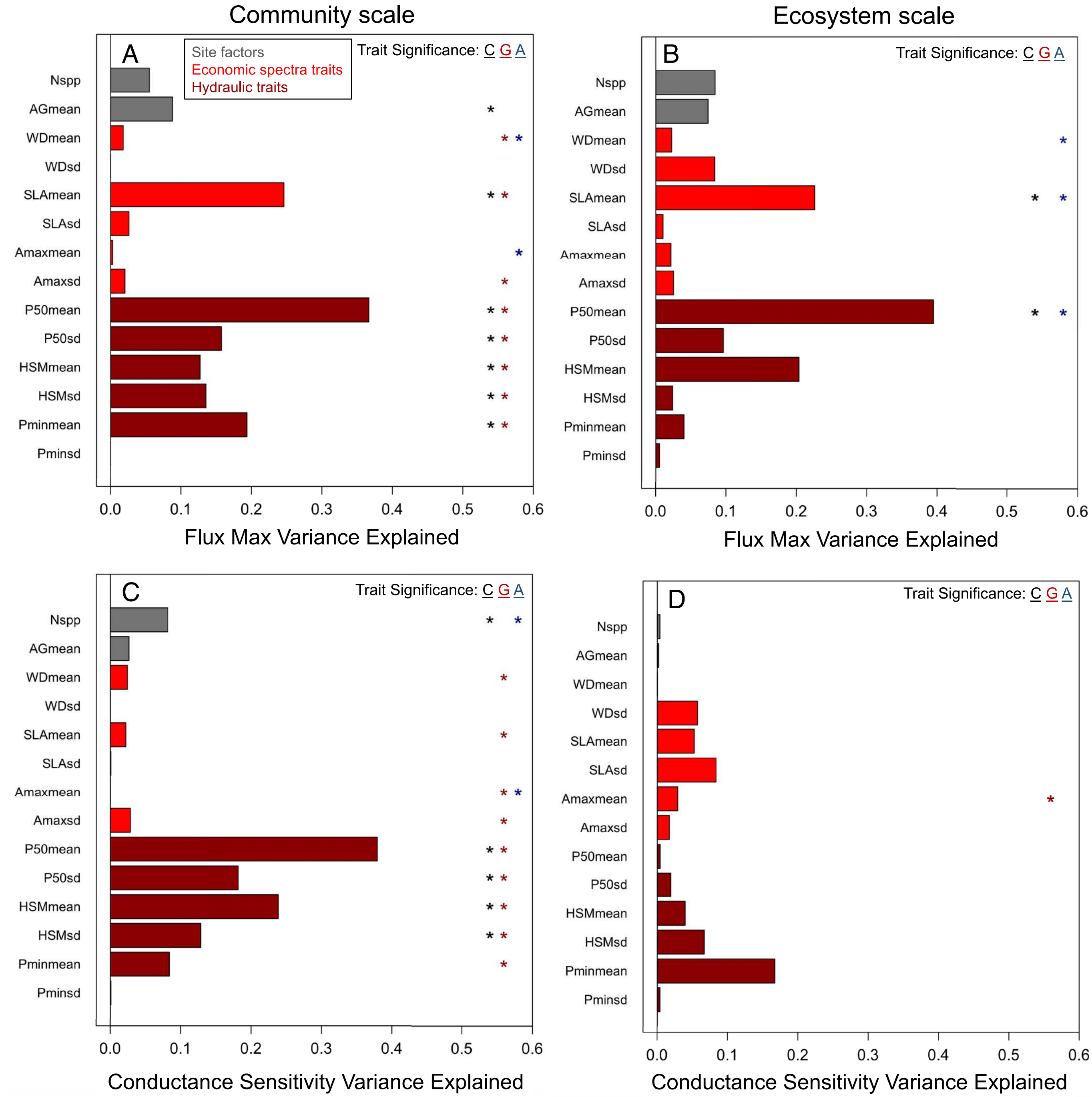

Fig. 3. Key traits that underpin flux scaling at community and ecosystem scales. Variance explained (R^2) between univariate community-weighted traits versus maximum water fluxes (*A* and *B*) or sensitivity of canopy conductance to VPD (*C* and *D*) at community (*A* and *C*) or ecosystem (*B* and *D*) scales. Site Metrics include species richness (Nspp) and fraction of forest composition that is gymnosperm species (AGmean). Traits include the community-weighted mean and SD of WD, SLA, maximum photosynthesis rate (Amax), water potential at which 50% of hydraulic conductivity is lost (P50), HSM, and minimum water potential (PsiM). Stars indicate statistically significant regressions ($P < 0.05$ after correction for multiple hypothesis testing) for combined species (C, black), gymnosperm-dominated sites (G, red), and angiosperm-dominated sites (A, blue).

maximum flux rates than for the sensitivity of canopy conductance to VPD.

Why does the conservative-acquisitive trade-off that is so striking at a species scale largely disappear at the ecosystem scale? We hypothesized that community assembly processes of environmental filtering (22) and niche partitioning (19) that influence species and trait diversity over long time scales might weaken or decouple these trade-offs. We tested this by including community-weighted traits as covariates in the trade-off regression model and examining i) the change in Akaike Information Criterion (AIC) between the no-trait vs. trait-included models, where a ΔAIC < −3 indicates that the trait-included model is meaningfully more likely given the data, and ii) the significance of the interaction term between the trait and independent variable, indicating that the trait mediates the trade-off. At the community scale, four community-weighted mean functional traits (SLA, WD, maximum photosynthetic rate, and minimum measured water potential) and species richness improved model fit (ΔAIC < −3) (Fig. 5). Species richness and WD exhibited significant interaction terms (richness $P_{adj} = 0.002$, WD $P_{adj} < 0.0001$), whereby lower wood densities and higher number of species showed a shallower, less tight conservative-acquisitive trade-off (Fig. 5). We found that many more traits showed significant

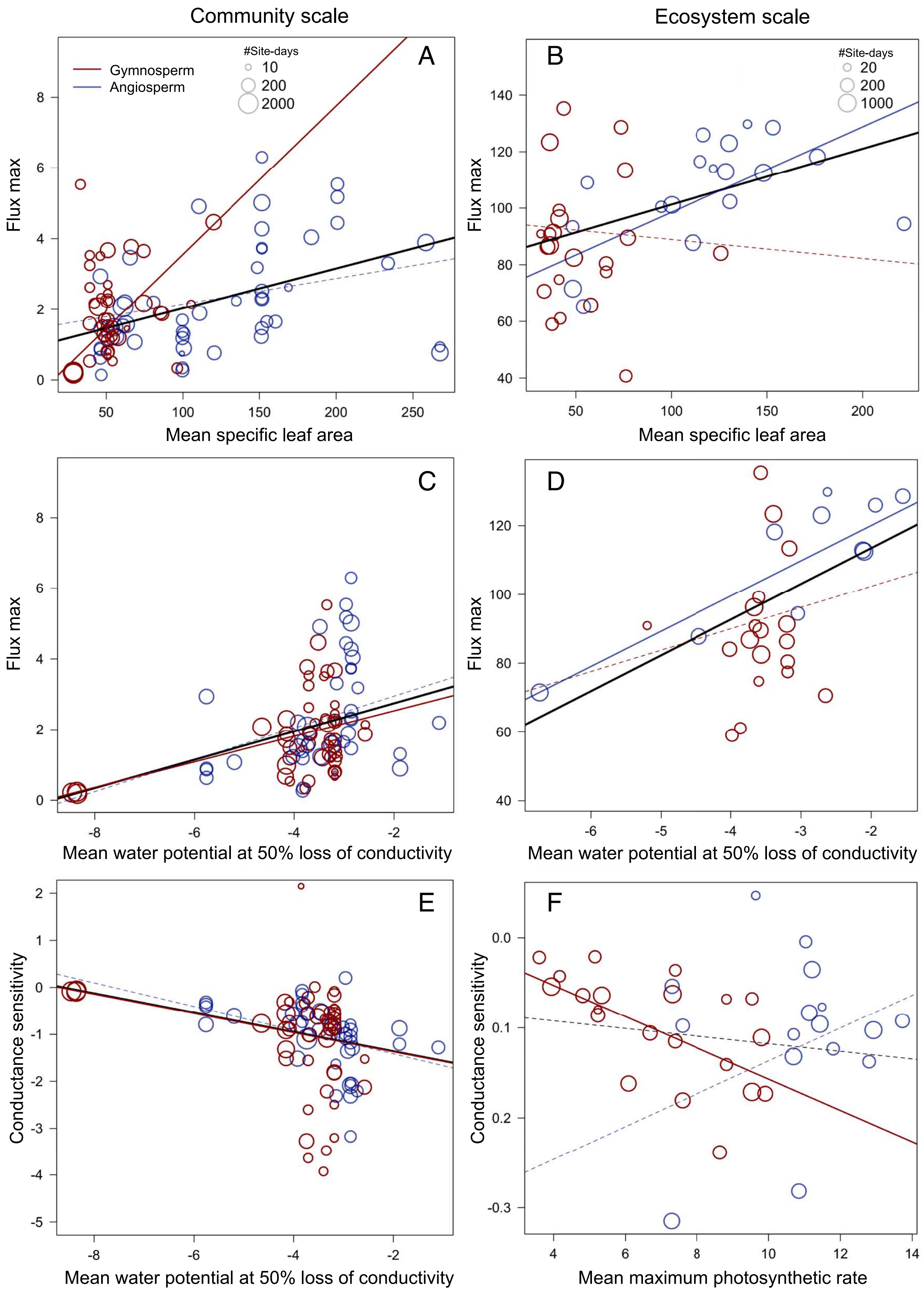

Fig. 4. Trait versus community and ecosystem flux responses highlight hydraulic and Leaf Economic Spectrum (LES) traits. Panels (*A*–*D*) show the maximum water fluxes and Panels (*E* and *F*) show the sensitivity of canopy conductance to VPD. Univariate relationships between community-weighted traits and community (*A*, *C*, and *E*) or ecosystem (*B*, *D*, and *F*) flux responses. Maximum water flux units are mm/d (*A* and *C*), average daily W/m^2 latent heat fluxes (*B* and *D*), and conductance sensitivity units are mm/(day log(kPa)) (*E*), and mol water/(m^2 s kPa) (*F*). Blue circles indicate angiosperm species or angiosperm-dominated sites and the blue line is the ordinary least squares regression for those species/sites. Red circles indicate gymnosperm species or gymnosperm-dominated sites and the red line is the ordinary least squares regression for those species/sites. The black line is all species/sites. Circle size is proportionate to the number of tree-days or site-days for each species/site. Solid lines indicate statistical significance of the regression.

interaction terms at the species-level compared to the community-level, which provides evidence that trait scaling may be decoupling a conservative-acquisitive trade-off in the same dataset (*SI Appendix*, Fig. S3). At the ecosystem scale, a similar set of functional traits improved model fit in terms of AIC, but we found no significant interaction terms (Fig. 4). Species richness and trait diversity were also significantly higher ($P < 0.01$ for richness and SD in WD, Amax, and P50 as example traits) at the ecosystem scale than community scale (*SI Appendix*, Fig. S3), supporting the hypothesis of environmental filtering driving increasing trait diversity as environmental heterogeneity increases. Notably, community-weighted mean traits were far more important in these analyses than trait diversity, which may further indicate a potential role for environmental filtering of community trait composition or that the number of species better captures the functional diversity than trait ranges in this dataset.

According to theory, functional diversity at community or ecosystem scales must be maintained by niche differentiation whereby different functional traits or strategies are favored at different microsites or time periods (24, 27, 37, 38). Individual species have evolved to show a specific combination of traits or a given life history strategy because no species can excel at both resource acquisition and stress tolerance due to biophysical constraints and trade-offs (1, 2, 19, 38). However, 6 communities and ecosystems do not have to "choose" a strategy. Instead, ecosystems are composed of species with a wide array of strategies and these species likely contribute differentially to ecosystem responses at different times (asynchrony), due to their differential sensitivity to environmental factors (Fig. 1) (23–27). Precisely because there is a trade-off between maximum fluxes and sensitivity to VPD at the species-level, we expect that acquisitive species on wetter microsites may contribute more to ecosystem maximum fluxes, while

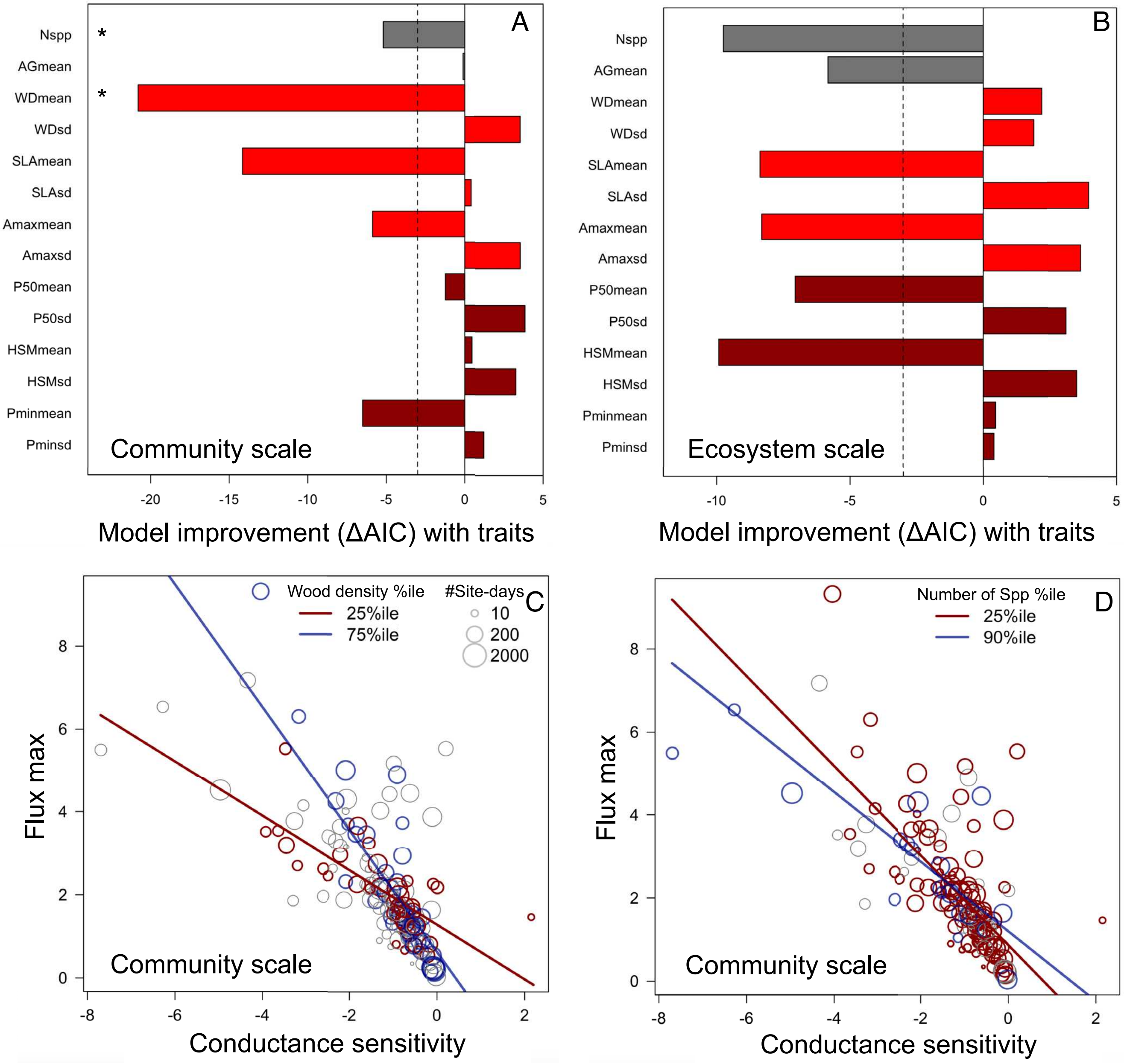

Fig. 5. Species richness and traits partially decouple conservative-acquisitive trade-offs. Panels (*A* and *B*) display the change in ΔAIC of a conservative-acquisitive ordinary least squares linear regression with a given functional trait versus without, with values of less than −3 (vertical dashed line) indicating a meaningful improvement to the model, for community (*A*) and ecosystem (*B*) scales. Stars (*) indicate the traits where the interaction term between the trait and the conductance sensitivity is statistically significant ($P_{adj} < 0.05$) after adjusting for multiple comparisons. Panels (*B* and *D*) display the conservative-acquisitive trade-off at the community scale as in Fig. 1*B*, but with low and high percentiles of WD (*C*) and species richness (Nspp; *D*) highlighted in colors. Maximum water flux units are mm/d (*C*), and average daily W/m^2 of latent heat fluxes (*D*) and conductance sensitivity units are mm/(day log(kPa)) (*C*) and mol water/(m^2 s kPa) (*D*). Lines are the ordinary least squares regression line for 25%ile and below points and 75%ile and 90%ile and above points, respectively. Solid lines indicate statistically significant regressions. Percentile cut-offs were based on the assessment of the respective data distributions.

more conservative species on less favorable microsites would dominate canopy conductance in the face of high VPD levels (Fig. 1) (9, 22). Our results that different functional traits are associated with maximum fluxes versus conductance sensitivities support this mechanism, as does a supplementary analysis of changes in the proportion of canopy conductance composed of different species as VPD increases (Fig. 3 and *SI Appendix*, Fig. S8). Indeed, an underappreciated finding of the seminal leaf economic spectrum paper (2) highlighted that the leaf trait diversity found within individual communities often spans much of the global spectrum space. In addition to dampening ecosystem trade-offs, community assembly processes may also work to strengthen the species-level trade-offs documented here because all species-level measurements are made on the realized niche (rather than the fundamental niche) and it is expected that competition has likely restricted species to the microsites and times where their strategies are most favorable (22, 37).

We posit several major implications of these results for scaling and improving ecosystem models under future climate scenarios. First, our results underscore that plant hydraulic traits hold potential for explaining functional responses across organizational scales, including both maximum fluxes and conductance sensitivity to VPD (9, 32, 39, 40). Second, our trait–response correlations (Fig. 3) reveal that both economic spectrum and hydraulic functional traits may be more useful for improving models of flux maximums than drought sensitivity patterns, extending beyond previous studies aiming to explore traits-ecosystem flux relationships that have not included hydraulic traits or considered species, community, and ecosystem scales together (12, 13, 41). Thus, identifying critical trait syndromes/functional axes underpinning whole-ecosystem sensitivity to drought stress and general metrics of drought sensitivity from flux dynamics are key model development avenues. Third, we find evidence that community assembly processes appear to buffer conservative-acquisitive trade-offs at large scales, which emphasizes that ecoevolutionary dynamics and improvements in community ecology that capture assembly as a driver of functional diversity, in addition to functional traits and ecophysiology, may be a promising pathway for improving ecosystem models.

We note several caveats in our analyses, including the use of species-average functional traits, the incomplete coverage of our flux datasets that lacks representation in tropical forests, limited temporal coverage of flux datasets that may not include severe drought conditions in some cases, canopy coupling assumptions, and that the sap flux and eddy covariance data differ in sample size and come from different geographic sites. These data-limitation-based caveats highlight important gaps for future research. Given generally quite similar geographic, climate, and temporal (record length) coverage of sap flux and eddy covariance sites (*SI Appendix*, Figs. S5 and S6), we do not believe that our central findings are likely to be greatly influenced by site differences and we observed similar patterns in a sensitivity analysis restricting sap flux sites to the same climate space covered by eddy covariance sites (*Methods*). The occurrence of a statistically significant ecosystem-level trade-off at gymnosperm-dominated sites (Fig. 1*C*), while still weaker than the species-level and community-level patterns, may indicate that boundary layer effects could partially explain weakening trade-offs at angiosperm-dominated sites, as gymnosperm canopies tend to be much more strongly coupled to the atmosphere (42). We did not observe significant ecosystem-level trade-offs using carbon flux metrics [gross primary productivity (GPP); *SI Appendix*, Fig. S1], however, in either clade, which indicates this weakening pattern is pervasive.

Ecosystem fluxes also include fluxes from understory species, whose traits were not analyzed here, and the niche partitioning of light between understory and overstory is another community assembly process that is likely to further contribute to the weaker trade-off documented here. Substantial literature has documented that understory plant communities can contribute ~10 to 50% or more of carbon and water fluxes, depending on the system, and that the diurnal and seasonal variation and sensitivity of understory fluxes to environmental conditions can diverge from that of the overstory (43–48). Thus, we posit that better estimation and measurement of understory fluxes and traits could be important for constraining and modeling of whole-ecosystem responses to VPD variation.

Trait-based ecology is predicated on the promise of using functional traits to predict ecological outcomes and there is enormous interest in using plant economic spectra to improve ecosystem models and reduce uncertainty in future carbon cycle projections. Conservative-acquisitive trade-offs provide a foundation for linking traits to large-scale ecosystem responses, but the scaling of these trade-offs has not previously been directly tested nor the role of which traits matter for which ecosystem responses been illuminated. We reveal here that a strong species-level trade-off dramatically weakens by ecosystem scales and that community-level plant hydraulic traits are strongly associated with community and ecosystem flux responses. Furthermore, this trade-off at the community-level varies with species richness, and species richness is one of the most important variables at the ecosystem scale. Our results indicate that in addition to improved physiological realism, better representation of community ecological processes—which are now increasingly possible in demographic vegetation models—may be equally crucial to improved understanding and projections of forest responses to climate change in the 21st century.

Methods

Datasets. We used previously published functional trait data by refs. 9 and 40, initially sourced from the TRY (49) and Hydra-TRY (50) datasets, for species present at the sap flux or eddy covariance sites. These two previous studies conducted careful evaluation of the source, measurement type (especially for plant hydraulic traits), and screening for any potential artifacts or erroneous values. These published trait datasets are based on mature, field-grown plants for the functional traits: WD (g/cm^3), SLA (cm^2/g), maximum light-saturated photosynthetic rate per unit leaf area [Amax, umol/(m^2*s)], the water potential at which 50% of stem hydraulic conductivity is lost (P50; MPa), the minimum stem water potential typically experienced by a species (PsiMin; MPa), and the HSM, defined as the PsiMin-P50 (MPa). Following previous studies, we generally restricted hydraulic trait data to standard methods (benchtop dehydration, air injection, and centrifuge methods) and took care to avoid the possibility of artifactual vulnerability curves (9). WD, SLA, and Amax are among the most commonly used "plant economic spectra" traits. For example, higher SLA and Amax are frequently considered more "acquisitive" species and are often linked to faster growth (1, 51). P50, PsiMin, and HSM are among the most widely used plant hydraulic traits. P50 frequently captures the degree of drought tolerance of species across environments (52).

We used a recently developed, cross-biome dataset of sap flux [SAPFLUXNET (34)]. Sap flow probes measure the velocity of water movement through stems and thus ideally capture key components of conservative-acquisitive trade-offs at an individual plant level, particularly the maximum water flux rates of transpiration and how transpiration responds to abiotic stress, such as VPD. At the species-level, we used the dataset of Flo et al. (2021) (40) that had carefully quality-controlled this dataset to ensure comparability across species and sites (40). This dataset included 170 species and 165 individual sites (*SI Appendix*, Fig. S7). All data analysis was conducted on daily data.

For ecosystem scale fluxes, we used the FLUXNET2015 dataset (35). We selected only forested sites that were undisturbed and largely unmanaged (i.e., sites that had not had a disturbance during and in the 10 y prior to flux measurements), to avoid impacts of severe disturbance and rapidly recovering/dynamic vegetation, and had >80% coverage (in basal area) in at least one functional trait, following previous research (9). We considered forested sites as those with the International Geosphere-Biosphere Programme biome designation in FLUXNET2015 of evergreen needleleaf forest, evergreen broadleaf forest, deciduous broadleaf forest, or mixed forest. This dataset included 40 sites that spanned multiple biomes in temperate, Mediterranean, and boreal forests (*SI Appendix*, Fig. S6) but did not include tropical forests due to functional trait coverage gaps. The lack of tropical forests in our analysis means that we are unable to quantify the ecosystem-level trade-off across the full climate space and species diversity ranges of Earth's forests and that additional community assembly processes that are thought to be important in tropical forests (17, 18) cannot be directly tested here. We note that a previous study using remote-sensing of canopy water content dynamics found shallower slopes between diurnal and seasonal canopy water content variation and woody plant species richness (9), indicating that tropical forests may exhibit an even weaker trade-off, but more work is needed.

We note that the geographic and climate coverage of these two datasets is broadly similar (*SI Appendix*, Fig. S6), indicating that comparing trade-offs between the two datasets is unlikely to be driven by differential biome coverage. Similar to the sapflux data, all data analysis was conducted on daily data. We further did a sensitivity analysis (see below) where we restricted the datasets to the exact same climate space to verify that our findings were robust.

Data Processing. We calculated the community-weighted mean and SD of all functional traits for each sapflux or eddy covariance site using the basal area contribution of each species. In some instances for eddy covariance sites, we used reported species composition estimates by the underlying primary literature on those sites. For important site metrics, we also compiled species richness of tree species at the site and the fraction of the site basal area that corresponds to gymnosperm species. In previous work at these sites, we compiled stand age, but this variable was not important in those drought analyses and thus is not included here (9). Community-level sapflux was obtained by calculating mean species sapflux per basal area and then multiplying by each species' basal area in each stand as described in ref. 53. We filtered out days with low temporal coverage (i.e., there is a species representing >50% of the basal area, for which species transpiration has been estimated with less than 2 trees during a given day) or when the percentage of hourly timestamps with data was below 80% for a given day.

Finally, for both sapflux and eddy covariance data, we screened data before starting analyses by several criteria to ensure that we were analyzing the plant-active season (e.g., "growing season") and days with adequate conditions to drive transpiration (sapflux) or days where transpiration is likely to dominate latent heat fluxes (eddy covariance data). Following previous studies for these screening criteria (40), we excluded days where daytime average VPD < 0.3 kPa, rainy days (detected via rapid soil water content increases), and plant-active season thresholds defined in Flo et al. (2021) for sapflux data. For eddy covariance data, following previous studies (9, 54), we excluded days where VPD < 0.5 kPa, photosynthetic photon flux density < 100 μmol photons/(m^2*s), and daily precipitation > 2 mm. We furthermore only examined days where average temperatures exceeded 5 °C to determine plant-active season. While these screening criteria are not identical, they were chosen to be consistent with previous analyses on these datasets and we conducted multiple sensitivity analyses on VPD and temperature thresholds and observed very little change in our key conservative-acquisitive trade-off metrics used in all analyses.

Calculating Conservative-Acquisitive Trade-Offs. To estimate the level of acquisitiveness of a given species, community, or ecosystem, we calculated the maximum flux rate as the 90%ile of sapflux or latent heat fluxes for that species, community, or ecosystem. This approach is based on previous analyses (14) and is strongly analogous to Amax at the leaf-level for capturing acquisitiveness. To estimate the drought sensitivity or tolerance of a given species, community, or ecosystem, we quantified the sensitivity of canopy conductance to VPD using the regression coefficient between canopy conductance and VPD. This approach has been widely used at the leaf, tree, and ecosystem scale in other analyses (39, 40, 55, 56). We calculated canopy conductance in sapflow data as the daily average transpiration/average VPD following Darcy's law. For eddy covariance data, we used the method derived in Wehr and Saleska (2021) (57) that uses both latent and sensible heat fluxes and flux gradient equations to derive canopy conductance, which has been shown to be more flexible, rigorously grounded, and accurate than the typical inversion of Penman–Montieth equations (57).

We constructed ordinary least squares linear regressions between canopy conductance and either the natural log of VPD for sap flux data or untransformed VPD for eddy covariance data, which was supported both by our exploratory analysis as better fits for each dataset and the common transformation used in the literature (39, 40). As a sensitivity analysis, we also calculated the canopy conductance sensitivity with the natural log of VPD for eddy covariance data and found very similar patterns (*SI Appendix*, Fig. S7).

To quantify whether trait means or trait variation might influence the scaling of the trade-off (Fig. 5), we constructed ordinary least squares linear regressions similarly to Fig. 2 but with each trait variable sequentially included as a predictor with an interaction term (i.e., maximum fluxes as the dependent variable and the independent variables as conductance sensitivity, trait mean or SD, and the interaction between conductance sensitivity and the trait variable). We evaluated the influence in traits using the change in AIC of the linear regression model with versus without the trait predictor and the significance of the interaction term. We analyzed all forested sites considered together, and we also tested angiosperm-dominated and gymnosperm-dominated sites as additional analyses in Figs. 2–4. We conducted this clade-specific analysis because it is common practice in both trait and flux studies (1, 9, 10, 40–42) and differential trait–function relationships may be expected due to large differences in physiology, canopy structure, and boundary layer conditions (9, 10, 12, 42). A site was classified as "gymnosperm-dominated" if more than 50% of its composition (typically basal area or stem density) was from gymnosperm species following previous studies (9, 40). We further note that we included the fraction of a site that is gymnosperm in our regression analyses in Fig. 3, which directly incorporates the degree of angiosperm-gymnosperm mixed forests into our analyses.

Sensitivity Analyses. We conducted several sensitivity analyses to ensure that our metrics capturing the conservative-acquisitive trade-off were robust. First, we compared our eddy covariance metrics of maximum latent heat flux and sensitivity of canopy conductance to VPD to the same metrics calculated using the nighttime partitioning method (58) of GPP. We found strong correlations in both metrics ($r = 0.69$, $r = 0.53$, $P \ll 0.00001$ for both) (*SI Appendix*, Fig. S2), and we noted that there was no significant correlation between maximum fluxes and flux sensitivities to VPD in the GPP metrics ($P = 0.14$), further supporting our main conclusions. Second, we included soil moisture as a covariate in our regression models for both sapflux and eddy covariance data at sites where it was included and observed strongly correlated patterns in the VPD sensitivity coefficients between models with versus without soil moisture ($r_{comm} = 0.94$, $r_{ecos} = 0.92$, $P \ll 0.00001$ for both) (*SI Appendix*, Fig. S2). These analyses underscore that our primary metrics are likely robust and not likely confounded by not explicitly modeling soil moisture impacts. Third, we calculated the fractional contribution of each species to overall community canopy conductance as VPD increases in the 10 SAPFLUXNET sites with at least two species and 3 y of complete data and found differential slopes in 90% of those sites and rank-order changes in 50% of sites (*SI Appendix*, Fig. S8), supporting a buffering effect as species richness increases. Finally, we subsampled the species and community-level SAPFLUXNET data to the same climate space as FLUXNET2015 sites (MAP [480,1,600] mm, MAT [−3, 26] °C from *SI Appendix*, Fig. S6) and verified that similar trade-offs were observed in this subsample ($N_{\text{species}} = 93$, $R^2_{\text{species}} = 0.49$, $p_{\text{species}} \ll 0.00001$; $N_{\text{comm}} = 88$, $R^2_{\text{comm}} = 0.53$, $p_{\text{comm}} \ll 0.00001$), such that the weakening trade-off at ecosystem scales is not likely due to a restricted climate space in eddy covariance sites.

Statistics and Availability of Data and Code. We conducted all trait–flux analyses as ordinary least square linear regression models, although we verified that the scaling trade-off patterns observed in Fig. 2 were robust to analysis via a type II regression (RMA: $p_{\text{species}} < 0.01$; $p_{\text{comm}} < 0.01$; $p_{\text{ecosystem}} = 0.08$). For

Figs. 3 and 5, we conducted a *P*-value correction for multiple hypothesis testing per Holm's method (59). This method is a fairly stringent (conservative) method of adjustment of *P*-values and *P*-values denoted as "P_{adj}" in the main text indicate where this correction was applied. We compared species richness and trait diversity (community-weighted trait SD of WD, Amax, and P50) between community and ecosystem scales using *t* tests for means and Kolmogorov–Smirnov tests for distribution differences. All analyses were conducted in the R statistical environment (R Core Team 2012).

SAPFLUXNET data version 0.1.6 used here can be reproduced by running the code at <https://github.com/sapfluxnet/sfn_0_1_5_corrections> on the data available at Zenodo <https://doi.org/10.5281/zenodo.3971689> <rep 0.1.5>. FLUXNET2015 Tier 1 data used in the study are available at <https://fluxnet.org/data/fluxnet2015-dataset/>. All trait data are publicly available from previous studies (8, 40). Code used to undertake this analysis can be found at https://doi.org/10.6084/m9.figshare.23137193 (60).

Data, Materials, and Software Availability. Code have been deposited in FigShare https://doi.org/10.6084/m9.figshare.23137193 (60). Previously published data were used for this work (https://doi.org/10.5281/zenodo.3971689 (61) and https://fluxnet.org/data/fluxnet2015-dataset/) (35). All other data are included in the article and/or *SI Appendix*.

ACKNOWLEDGMENTS. W.R.L.A. acknowledges the support from the David and Lucille Packard Foundation, Severo Ochoa Excellence Program (CEX2018-000828-S), US NSF grants 1802880, 2003017, 2044937, and Alan T. Waterman Award IOS-2325700. R.P. acknowledges the Ministerio de Ciencia e Innovación (grant no. RTI2018-095297-J-I00), and the Alexander von Humboldt-Stiftung [Humboldt Research Fellowship for Experienced Researchers (R.P.)]. J.M.-V. acknowledges the Agència de Gestió d'Ajuts Universitaris i de Recerca de Catalunya (grant 2021 SGR 00849) and the Institució Catalana de Recerca i Estudis Avançats (ICREA Academia award).

1. P. B. Reich, The world-wide 'fast–slow' plant economics spectrum: A traits manifesto. *J. Ecol.* **102**, 275–301 (2014).
2. I. J. Wright *et al.*, The worldwide leaf economics spectrum. *Nature* **428**, 821–827 (2004).
3. S. Díaz *et al.*, The global spectrum of plant form and function. *Nature* **529**, 167–171 (2016).
4. M. Migliavacca *et al.*, The three major axes of terrestrial ecosystem function. *Nature* **598**, 468–472 (2021).
5. B. J. McGill, B. J. Enquist, E. Weiher, M. Westoby, Rebuilding community ecology from functional traits. *Trends Ecol. Evol.* **21**, 178–185 (2006).
6. P. B. Adler *et al.*, Functional traits explain variation in plant life history strategies. *Proc. Natl. Acad. Sci. U.S.A.* **111**, 740–745 (2013).
7. N. J. Kraft, O. Godoy, J. M. Levine, Plant functional traits and the multidimensional nature of species coexistence. *Proc. Natl. Acad. Sci. U.S.A.* **112**, 797–802 (2015).
8. R. A. Fisher *et al.*, Vegetation demographics in Earth System Models: A review of progress and priorities. *Glob. Change Biol.* **24**, 35–54 (2018).
9. W. R. Anderegg *et al.*, Hydraulic diversity of forests regulates ecosystem resilience during drought. *Nature* **561**, 536–541 (2018).
10. L. D. Anderegg *et al.*, Within-species patterns challenge our understanding of the leaf economics spectrum. *Ecol. Lett.* **21**, 734–744 (2018).
11. M. Reichstein, M. Bahn, M. D. Mahecha, J. Kattge, D. D. Baldocchi, Linking plant and ecosystem functional biogeography. *Proc. Natl. Acad. Sci. U.S.A.* **111**, 13697–13702 (2014).
12. N. He *et al.*, Predicting ecosystem productivity based on plant community traits. *Trends Plant Sci.* **28**, P43–P53 (2022).
13. U. Gomarasca *et al.*, Leaf-level coordination principles propagate to the ecosystem scale. *Nat. Commun.* **14**, 3948 (2023).
14. S. Manzoni *et al.*, Hydraulic limits on maximum plant transpiration and the emergence of the safety–efficiency trade-off. *New Phytol.* **198**, 169–178 (2013).
15. D. D. Ackerly, W. K. Cornwell, A trait-based approach to community assembly: Partitioning of species trait values into within- and among-community components. *Ecol. Lett.* **10**, 135–145 (2007).
16. N. J. B. Kraft, R. Valencia, D. D. Ackerly, Functional traits and niche-based tree community assembly in an Amazonian forest. *Science* **322**, 580–582 (2008).
17. C. X. Garzon-Lopez, P. A. Jansen, S. A. Bohlman, A. Ordonez, H. Olff, Effects of sampling scale on patterns of habitat association in tropical trees. *J. Veg. Sci.* **25**, 349–362 (2014).
18. S. P. Hubbell, Neutral theory and the evolution of ecological equivalence. *Ecology* **87**, 1387–1398 (2006).
19. E. Weiher *et al.*, Advances, challenges and a developing synthesis of ecological community assembly theory. *Philos. Trans. R. Soc. B Biol. Sci.* **366**, 2403–2413 (2011).
20. R. Perronne, F. Munoz, B. Borgy, X. Reboud, S. Gaba, How to design trait-based analyses of community assembly mechanisms: Insights and guidelines from a literature review. *Perspect. Plant Ecol. Evol. Syst.* **25**, 29–44 (2017).
21. C. P. Carmona, F. De Bello, N. W. Mason, J. Lepš, Traits without borders: Integrating functional diversity across scales. *Trends Ecol. Evol.* **31**, 382–394 (2016).
22. N. J. Kraft, D. D. Ackerly, Assembly of plant communities. *Ecol. Environ.* **8**, 67–88 (2014).
23. D. Tilman, D. Wedin, J. Knops, Productivity and sustainability influenced by biodiversity in grassland ecosystems. *Nature* **379**, 718–720 (1996).
24. D. Tilman, P. B. Reich, J. M. Knops, Biodiversity and ecosystem stability in a decade-long grassland experiment. *Nature* **441**, 629–632 (2006).
25. N. Rooney, K. McCann, G. Gellner, J. C. Moore, Structural asymmetry and the stability of diverse food webs. *Nature* **442**, 265–269 (2006).
26. A. Hector *et al.*, General stabilizing effects of plant diversity on grassland productivity through population asynchrony and overyielding. *Ecology* **91**, 2213–2220 (2010).
27. M. Loreau, C. De Mazancourt, Biodiversity and ecosystem stability: A synthesis of underlying mechanisms. *Ecol. Lett.* **16**, 106–115 (2013).
28. S. Scheiter, L. Langan, S. I. Higgins, Next-generation dynamic global vegetation models: Learning from community ecology. *New Phytol.* **198**, 957–969 (2013).
29. P. Friedlingstein *et al.*, Uncertainties in CMIP5 climate projections due to carbon cycle feedbacks. *J. Clim.* **27**, 511–526 (2014).
30. A. D. Friend *et al.*, Carbon residence time dominates uncertainty in terrestrial vegetation responses to future climate and atmospheric CO2. *Proc. Natl. Acad. Sci. U.S.A.* **111**, 3280–3285 (2013), 10.1073/pnas.1222477110.
31. C. B. Eller *et al.*, Stomatal optimization based on xylem hydraulics (SOX) improves land surface model simulation of vegetation responses to climate. *New Phytol.* **226**, 1622–1637 (2020).
32. M. E. Sabot *et al.*, Plant profit maximization improves predictions of European forest responses to drought. *New Phytol.* **226**, 1638–1655 (2020).
33. S. I. Higgins, S. Scheiter, Atmospheric CO2 forces abrupt vegetation shifts locally, but not globally. *Nature* **488**, 209–212 (2012).
34. R. Poyatos *et al.*, Global transpiration data from sap flow measurements: The SAPFLUXNET database. *Earth Syst. Sci. Data* **13**, 2607–2649 (2021).
35. G. Pastorello *et al.*, The FLUXNET2015 dataset and the ONEFlux processing pipeline for eddy covariance data. *Sci. Data* **7**, 225 (2020), https://doi.org/10.1038/s41597-020-0534-3.
36. C. Grossiord *et al.*, Plant responses to rising vapor pressure deficit. *New Phytol.* **226**, 1550–1566 (2020).
37. J. Silvertown, Y. Araya, D. Gowing, Hydrological niches in terrestrial plant communities: A review. *J. Ecol.* **103**, 93–108 (2015).
38. K. Jops, J. P. O'Dwyer, Life history complementarity and the maintenance of biodiversity. *Nature* **618**, 986–991 (2023).
39. R. Oren *et al.*, Survey and synthesis of intra- and interspecific variation in stomatal sensitivity to vapour pressure deficit. *Plant Cell Environ.* **22**, 1515–1526 (1999).
40. V. Flo *et al.*, Climate and functional traits jointly mediate tree water use strategies. *New Phytol.* **231**, 617–630 (2021).
41. H. Xu, Z. Zhang, R. Oren, X. Wu, Hyposensitive canopy conductance renders ecosystems vulnerable to meteorological droughts. *Global Change Biol.* **29**, 1890–1904 (2023).
42. M. G. De Kauwe, B. E. Medlyn, J. Knauer, C. A. Williams, Ideas and perspectives: How coupled is the vegetation to the boundary layer? *Biogeosciences* **14**, 4435–4453 (2017).
43. P. D. Blanken *et al.*, Energy balance and canopy conductance of a boreal aspen forest: Partitioning overstory and understory components. *J. Geophys. Res. Atmos.* **102**, 28915–28927 (1997).
44. E. H. Hogg *et al.*, Responses of trembling aspen and hazelnut to vapor pressure deficit in a boreal deciduous forest. *Tree Physiol.* **20**, 725–734 (2000).
45. L. Misson *et al.*, Partitioning forest carbon fluxes with overstory and understory eddy-covariance measurements: A synthesis based on FLUXNET data. *Agric. For. Meteorol.* **144**, 14–31 (2007).
46. S. Iida *et al.*, Evapotranspiration from understory vegetation in an eastern Siberian boreal larch forest. *Agric. For. Meteorol.* **149**, 1129–1139 (2009).
47. H. Ikawa *et al.*, Understory CO2, sensible heat, and latent heat fluxes in a black spruce forest in interior Alaska. *Agric. For. Meteorol.* **214**, 80–90 (2015).
48. E. Martínez-García *et al.*, Drought response of the boreal forest carbon sink is driven by understorey–tree composition. *Nat. Geosci.* **17**, 197–204 (2024).
49. J. Kattge *et al.*, TRY–A global database of plant traits. *Glob. Change Biol.* **17**, 2905–2935 (2011).
50. P. Sanchez-Martinez, J. Martínez-Vilalta, K. G. Dexter, R. A. Segovia, M. Mencuccini, Adaptation and coordinated evolution of plant hydraulic traits. *Ecol. Lett.* **23**, 1599–1610 (2020).
51. R. S. Oliveira *et al.*, Linking plant hydraulics and the fast–slow continuum to understand resilience to drought in tropical ecosystems. *New Phytol.* **230**, 904–923 (2021).
52. H. Maherali, W. T. Pockman, R. B. Jackson, Adaptive variation in the vulnerability of woody plants to xylem cavitation. *Ecology* **85**, 2184–2199 (2004).
53. R. M. Bright, D. G. Miralles, R. Poyatos, S. Eisner, Simple models outperform more complex big-leaf models of daily transpiration in forested biomes. *Geophys. Res. Lett.* **49**, e2022GL100100 (2022).
54. K. A. Novick *et al.*, The increasing importance of atmospheric demand for ecosystem water and carbon fluxes. *Nat. Clim. Change* **6**, 1023–1027 (2016).
55. D. E. Pataki, R. Oren, G. Katul, J. Sigmon, Canopy conductance of Pinus taeda, Liquidambar styraciflua and Quercus phellos under varying atmospheric and soil water conditions. *Tree Physiol.* **18**, 307–315 (1998).
56. G. Cai *et al.*, Transpiration response to soil drying and vapor pressure deficit is soil texture specific. *Plant Soil*, 10.1007/s11104-022-05818-2 (2022).
57. R. Wehr, S. R. Saleska, Calculating canopy stomatal conductance from eddy covariance measurements, in light of the energy budget closure problem. *Biogeosciences* **18**, 13–24 (2021).
58. G. Lasslop *et al.*, Separation of net ecosystem exchange into assimilation and respiration using a light response curve approach: Critical issues and global evaluation. *Glob. Change Biol.* **16**, 187–208 (2010).
59. S. Holm, A simple sequentially rejective multiple test procedure. *Scand. J. Stat.* **6**, 65–70 (1979).
60. W. R. L. Anderegg, J. Martinez-Vilalta, M. Mencuccini, R. Poyatoes, Code for "Community assembly mediates plant trait economic spectra at ecosystem scales". [Code] Figshare. https://doi.org/10.6084/m9.figshare.23137193. Deposited 29 May 2023.
61. R. Poyatos *et al.*, SAPFLUXNET: A global database of sap flow measurements (0.1.5) [Data set]. Zenodo. https://doi.org/10.5281/zenodo.3971689. Deposited 4 August 2020.